Available online at www.sciencedirect.com
ScienceDirect
Trans. Nonferrous Met. Soc. China 28(2018) 2248−2254
Transactions of Nonferrous Metals Society of China
www.tnmsc.cn

Preparation of three-dimensional braided carbon fiber reinforced mullite composites from a sol with high solid content

Wei ZHANG[1,2], Qing-song MA[2], Ke-wei DAI[2], Wei-guo MAO[1]

1. School of Materials Science and Engineering, Xiangtan University, Xiangtan 411105, China;
2. Science and Technology on Advanced Ceramic Fibers & Composites Laboratory, National University of Defense Technology, Changsha 410073, China

Received 28 August 2017; accepted 16 December 2017

Abstract: To prepare the three-dimensional braided carbon fiber reinforced mullite (3D C/mullite) composites, an Al_2O_3−SiO_2 sol with a solid content of 20% (mass fraction) and an Al_2O_3/SiO_2 mass ratio of 2:1 was selected as the raw material. Characteristics and mullitization of the sol were analyzed throughly. It is found that the formation of mullite is basically completed at 1300 °C and the gel powders exhibit favorable sintering shrinkage. The 3D C/mullite composites without interfacial coating were fabricated through the route of vacuum impregnation−drying−heat treatment. Satisfied mechanical properties with a flexural strength of 241.2 MPa and a fracture toughness of 10.9 MPa·m$^{1/2}$ are obtained although the total porosity reaches 26.0%. Oxidation resistances of the composites at 1200, 1400 and 1600 °C were investigated. Due to the further densification of matrix, the 3D C/mullite composites show tiny mass loss and their mechanical properties are well retained after oxidation at 1600 °C for 30 min.

Key words: carbon fiber reinforced mullite composites; Al_2O_3−SiO_2 sol; mechanical properties; oxidation resistance

1 Introduction

Mullite ceramics are well known as the high performance structural materials owing to their low density, low thermal expansion, desirable thermal stability, excellent oxidation resistance, and so on [1−4]. However, the wide applications of monolithic mullite ceramics are restricted because of their low fracture toughness (2−3 MPa·m$^{1/2}$). Of all the toughening methods, continuous fiber reinforcement is predominant because of its outstanding damage tolerance. So far, oxide fiber, SiC fiber and C fiber have been employed to reinforce mullite ceramics [5−11] and the oxide fibers are the most extensively used reinforcement.

Although carbon fiber has been extensively used to reinforce other ceramics, the study on the carbon fiber reinforced mullite composites has been rarely reported [10,11]. In the studies of WU et al [10,11], unidirectional (UD) carbon fiber tow was impregnated in a single stage by passing it through an Al_2O_3−SiO_2 sol and wound onto a hexagonal drum to form a sheet prepreg. After being dried, the prepregs were stacked and hot-pressed to obtain the UD C/mullite composites. The resulted composites showed high mechanical properties in *X* direction. However, the interlaminar strength and the in-plane strength were low due to the absence of carbon fiber in the *Y* and *Z* directions. Furthermore, this route is difficult for the fabrication of large-size parts with a complex shape.

Three-dimensional (3D) braided fiber preform is considered as a desirable reinforcement for high performance composite materials because of its flexibility in the structure design, desirable comprehensive performance and adaptability to the complex shape. In order to realize the homogeneous distribution of matrix and the low fabrication temperature, gas infiltration and solution impregnation routes are preferentially adopted to fabricate 3D fiber reinforced mullite composites, especially the large-size complex parts. Nevertheless, proper gaseous raw materials for Al_2O_3−SiO_2 co-deposition have not been

Foundation item: Project (SAST2015043) supported by the Science Innovation Foundation of Shanghai Academy of Spaceflight Technology, China; Project (614291102010117) supported by the Open Foundation of Science and Technology on Thermostructural Composite Materials Laboratory, China; Project (11572277) supported by the National Natural Science Foundation of China
Corresponding author: Qing-song MA, Tel: +86-731-84573168, Fax: +86-731-84576578, E-mail: nudtmqs1975@163.com; Wei-guo MAO, E-mail: ssamao@126.com
DOI: 10.1016/S1003-6326(18)64869-1

found so far. The ceramic yield from solution via sol-gel to Al_2O_3−SiO_2 is very low, leading to the 3D fiber reinforced mullite composites with high porosity and low strength [12].

Recently, several studies have reported fabrication of 3D braided oxide and SiC fiber preform reinforced Al_2O_3−SiO_2, ZrO_2−SiO_2 and SiO_2 composites [5−7,13,14] through the route of sol impregnation−drying−heat treatment (SIDH). The raw materials were sols with high solid content (20%−25%, mass fraction). The results indicate that the SIDH route is promising because it can improve the fabrication efficiency of the solution impregnation process and reserve the advantages of homogeneous distribution of matrix and low fabrication temperature. In this work, 3D braided carbon fiber reinforced mullite (C/mullite) composites were fabricated through the SIDH route, and the microstructure, mechanical properties and oxidation resistances of the composites were investigated.

2 Experimental

Three-dimensional braided carbon fiber preform with a fiber volume fraction of 45% was selected as the reinforcement. The fiber was ex-PAN carbon fiber with a trademark of T300 and a density of 1.76 g/cm^3. The Al_2O_3−SiO_2 diphasic sol with a solid content of 20% (mass fraction) and an Al_2O_3/SiO_2 mass ratio of 2:1 was used as the precursor for mullite matrix. The diameter of colloid particle in the sol was 20−30 nm. The pH value and viscosity of the sol were about 3.4 and 15.6 mPa·s, respectively. The SiO_2 is a little superfluous in the sol since the Al_2O_3/SiO_2 mass ratio of stoichiometric mullite ($3Al_2O_3·2SiO_2$) is 2.55:1. The sol was dried at 120 °C to obtain the gel powders.

After thermal treatment at 1400 °C for 1 h, the carbon fiber preform was impregnated with the sol under vacuum. Then, the preform was dried at 200 °C for 2 h after being soaked in the sol for 6 h, followed by heat treatment at 1400 °C for 1 h in inert atmosphere with a heating rate of 10 °C/min. After the cycle of impregnation−drying−heating was repeated 18 times, the C/mullite composites were obtained with a size of 70 mm (L) × 50 mm (W) × 4 mm (H). The as-received C/mullite composites were oxidized at various temperatures for 30 min under static air.

Fourier transformation infrared spectroscopy (FTIR) of the gel powders between 4000 and 400 cm^{-1} were carried out using the KBr disk method with a resolution of 4 cm^{-1}. Thermal analysis (STA 449C, Netzsch) of the gel powders was performed by simultaneous thermal gravimetric (TG) and differential scanning calorimetry (DSC) analysis with a heating rate of 10 °C/min. Phase compositions of the gel powders that were heated at different temperatures in inert atmosphere were determined by X-ray diffraction, which was carried out on a diffractometer (Bruker D8 advance) with Cu K_α radiation. The data were digitally recorded during a continuous scan in the range of angle (2θ) from 10° to 80° with a scanning rate of 4 (°)/min. At the same time, the gel powders were cold-pressed at 120 MPa to wafers, followed by heat treatment at various temperatures. The linear shrinkage and microstructures after heat treatment were measured and observed.

The apparent density (ρ_a) of C/mullite composites was computed from the mass-to-volume ratio. The bulk density and the open porosity were measured according to the Archimede's principle with deionized water as immersion medium. The true density (ρ_m) of matrix was measured on the powdered sample using a pycnometer. Then, the theoretic density (ρ_T) of C/mullite composites was calculated from the equation:

$$\rho_T=\varphi_f·\rho_f+\varphi_m·\rho_m \quad (1)$$

where φ_f and φ_m are volume fractions of the fiber and the matrix, respectively, and ρ_f and ρ_m are densities of the fiber and the matrix, respectively. Thus, the total porosity was equal to $1-(\rho_a/\rho_T)$ and the open porosity subtracted from the total porosity gives close porosity.

The as-received and the oxidized composites were machined into bars of 70 mm (L) × 5 mm (W) × 4 mm (H) for the flexural test. Three-point bending test was employed to evaluate the flexural strength and the elastic modulus of C/mullite composites with a span/height ratio of 15 and a cross-head speed of 0.5 mm/min. The as-received composites were machined into bars with a size of 40 mm (L) × 8 mm (W) × 4 mm (H) for the fracture toughness test. The fracture toughness was determined by the single edge notched beam (SENB) method with a cross-head speed of 0.05 mm/min and a span/height ratio of 4. The ratio of notch depth to specimen height was 0.50. Five specimens were tested to obtain the average flexural strength and fracture toughness. Mass loss and flexural strength retention after oxidation were recorded to characterize the oxidation resistance of C/mullite composites. Scanning electron microscopy (Quanta−200 EDAX) was employed to observe the microstructures of wafers and composites.

3 Results and discussion

3.1 Mullitization behavior of sol

FTIR spectrum of the gel powders is shown in Fig. 1. Based on the previous results [15,16], the peaks at 3000−3500 cm^{-1} and 1650 cm^{-1} belong to the adsorption and hydration of H_2O, respectively. The stretch and bend modes of Si—O are found at 1110 and 460 cm^{-1}, respectively. The peaks at 840 and 620 cm^{-1} are assigned

to the stretch and bend modes of Al—O, respectively. It is noted that the peaks at 2450 and 1400 cm^{-1} do not belong to the chemical bonds of mullite. They could be ascribed to the organic compounds in sol, for example, the dispersant and the surfactant. However, the composition is not clear since the sol was purchased merchandise.

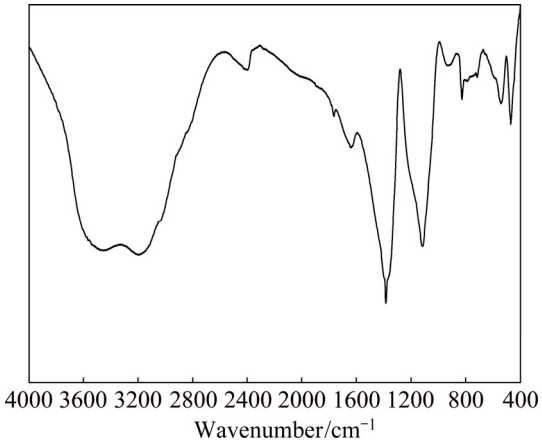

Fig. 1 FTIR spectrum of gel powders

Figure 2 illustrates the TG−DSC curves of the gel powders. A mass loss of ~7% resulting from the evaporation of residual water is found during room temperature to 120 °C. Accordingly, an endothermic peak at 100 °C is observed. Another mass loss of ~22% is detected from 120 to 270 °C, which can be ascribed to the dehydration of colloid and the decomposition of organic compounds. As a result, an endothermic peak at ~230 °C and two exothermic peaks at 180 and ~260 °C are noticed. The dehydration and decomposition is basically completed at 450 °C since the minute mass loss and faint caloric change are found above this temperature. An endothermic peak at 1140 °C and an exothermic peak at 1350 °C are observed above 450 °C. According to Ref. [16], the transformation from amorphous Al_2O_3 to γ-Al_2O_3 and the mullitization reaction are responsible for

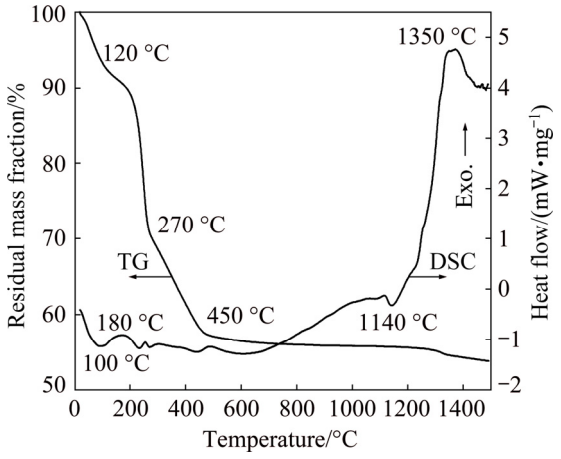

Fig. 2 TG−DSC curves of gel powders

the endothermic peak at 1140 °C and the exothermic peak at 1350 °C, respectively. Furthermore, the mullitization at 1350 °C indicates that the diphasic gel was obtained in this work [16].

Figure 3 presents XRD patterns of the gel powders after heat treatment at various temperatures. At 1000 °C, two faint peaks at ~22° and ~26° belonging to the rich SiO_2 and mullite, respectively, are observed. The emergence of the typical diffraction peaks of mullite at 1200 °C indicates a greater extent of the mullitization. As temperature increased, the crystallization of mullite is improved, as reflected by the gradually enhanced intensity. Especially, it is noted that the sharpness of the principal peak at ~26° is remarkably improved from 1400 to 1600 °C. At the same time, the intensity of diffraction peak of the rich SiO_2 is enhanced with increasing temperature from 1000 to 1400 °C, indicating the improvement in the crystallinity. At 1600 °C, the peak of rich SiO_2 is suppressed by the diffraction peaks of mullite.

Figures 4 and 5 show the linear shrinkage and SEM appearance of the gel powder wafers after heat treatment

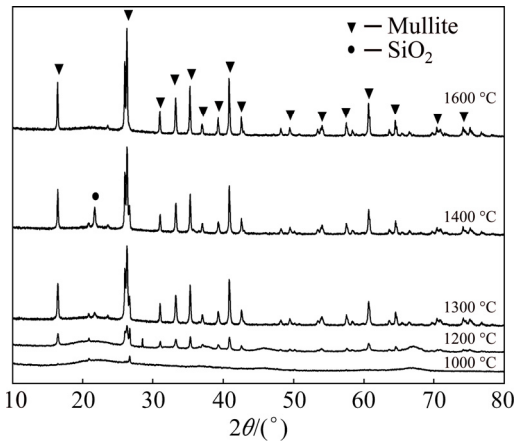

Fig. 3 XRD patterns of gel powders after heat treatment at different temperatures

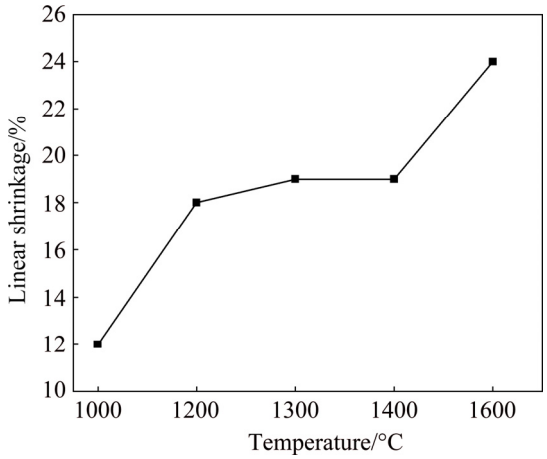

Fig. 4 Dependence of linear shrinkage of gel powder wafers on temperature

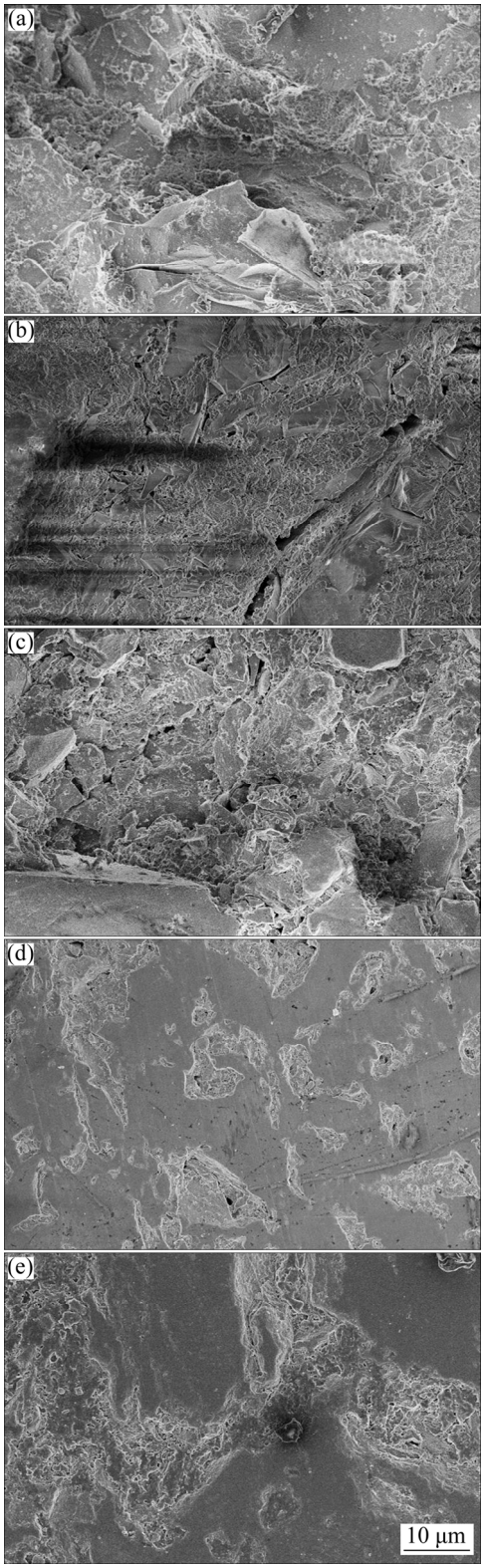

Fig. 5 SEM images of powder wafers after heat treatment at different temperatures: (a) 1000 °C; (b) 1200 °C; (c) 1300 °C; (d) 1400 °C; (e) 1600 °C

at various temperatures, respectively. Step-shaped linear shrinkage curve is observed in Fig. 4. A linear shrinkage of 12% is detected at 1000 °C, and this value is increased to ~18% at 1200 °C. The viscous flow of SiO_2 could account for this phenomenon. When the heat treatment was carried out above 1200 °C, most of the SiO_2 is consumed to create mullite and the crystallization of rich SiO_2 is enhanced, reducing the viscous flow effect. Accordingly, there is hardly any change in the linear shrinkage from 1200 to 1400 °C. At 1600 °C, the solid state sintering of mullite and rich SiO_2 is highly active, leading to obvious increment (~5%) in linear shrinkage. As shown in Fig. 5, uneven fracture surfaces with some cracks at 1000, 1200 and 1300 °C are converted to smooth and compact ones at 1400 and 1600 °C, which is due to the activated solid state sintering.

3.2 Microstructures, mechanical and anti-oxidation properties of 3D C/mullite composites

Based on the results of Figs. 3−5, the mullitization is almost completed and desirable densification is obtained at 1400 °C. Therefore, the heat treatment during the fabrication of C/mullite composites is carried out at 1400 °C. The as-received composites show an apparent density of 1.75 g/cm^3 and an open porosity of 12.0%. The true density (ρ_m) of matrix is measured to be 2.87 g/cm^3 and the theoretic density (ρ_T) of composites is calculated to be 2.37 g/cm^3. Thus, the total porosity and the close porosity are computed to be 26.0% and 14.0%, respectively.

Figure 6 shows the SEM appearances of the as-received composites. In Fig. 6(a), apart from several pores with a size of tens of micrometer, two or three large pores with a diameter of ~500 μm are obvious. These pores as well as some microcracks are observed in matrix. It is found from Fig. 6(b) that the intra-bundle spaces are well filled by matrix except few pores. It is easy for sol in initial cycles to infiltrate into preform and fill the intra- and inter-bundle spaces due to the low viscosity and the nanometer size. The space size is reduced and the diffusion channels to space become narrow and wandering with the increase of density of composites. Consequently, it is more and more difficult for sol to diffuse into composites, resulting in open and/or close pores. In addition, the viscous flow of rich SiO_2 during heat treatment is possible to obturate the diffusion channels, creating close pores. As for the large pores with a size of ~500 μm, it is very likely that they are created in the initial stage of densification. During the impregnation and soaking, it is impossible for sol to fill all the intra- and inter-bundle spaces. In the initial stage of densification, the intra-bundle spaces are preferentially occupied due to capillarity, whereas large size pores are probably formed in the inter-bundle. After heat treatment, these pores are closed by the viscous flow of rich SiO_2. Fortunately, these pores are not many. In subsequent study, pressure assisted impregnation and optimization of heat treatment will be performed to

lessen porosity and pore size, and remarkable improvement in mechanical properties can be anticipated.

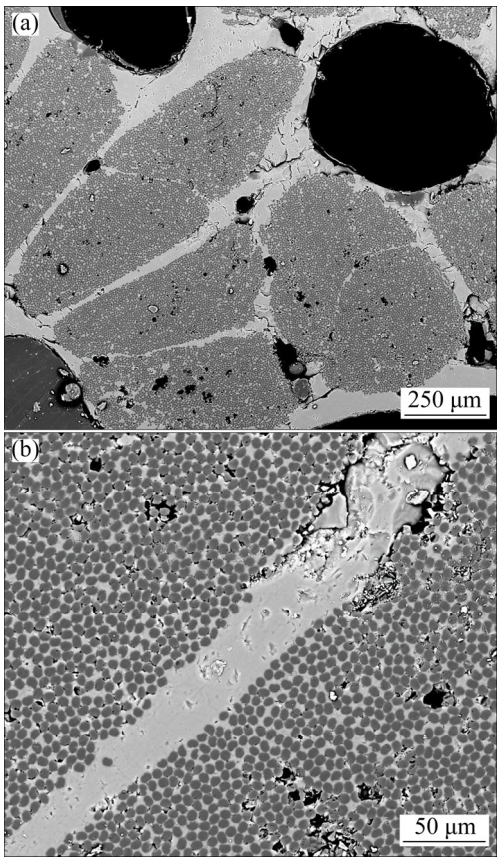

Fig. 6 SEM images of transverse section of as-received C/mullite composites

With regard to fiber reinforced ceramic matrix composites, the main function of ceramic matrix is to transfer the applied load to fiber, and interface plays a dominant role in deciding mechanical properties. If interfacial bonding is too weak and matrix is too loose, it is very difficult for the applied load to be transferred, leading to low flexural strength. On the contrary, brittle fracture behavior will be formed although load-transferring is effective. Moreover, if the strong interfacial bonding is created by the chemical reaction between matrix and fiber, in-situ strength of the carbon fibers is certain to be damaged to a great degree, resulting in the composites with low flexural strength and fracture toughness. Unfortunately, this is usual for fiber reinforced ceramic matrix composites due to the high temperature and/or the high pressure during densification. Only under the conditions of dense matrix and physically bonded interface with proper bonding strength, the high-performance composites can be obtained.

The mean flexural strength and the fracture toughness of fully dense monolithic mullite ceramics are ~300 MPa and 2−3 MPa·m$^{1/2}$, respectively. In this work, the as-received composites show a flexural strength of 241.2 MPa, an elastic modulus of 41.4 GPa and a fracture toughness of 10.9 MPa·m$^{1/2}$. Considering the high total porosity and the absence of interfacial coating, the mechanical properties are satisfying and have a great probability of improvement. In Fig. 7(a), a maximum displacement of ~1 mm at invalidation point is observed, which is much larger than that of monolithic ceramics (~0.2 mm). In Fig. 7(b), the fiber pull-out is obvious. These indicate that the interfacial bonding is not too strong. The crack-tip energy can be dissipated by fiber pull-out. Accordingly, the fracture toughness of monolithic mullite ceramics is remarkably enhanced to 10.9 MPa·m$^{1/2}$. However, the approximately vertical decline of load after invalidation point is found in Fig. 7(a). In Fig. 7(b), a relatively flat fracture surface with insufficient fiber pull-out and short pull-out length is observed. These brittle fracture characteristics suggest that the interfacial bonding is a little strong, which could be ascribed to the thermal stress due to the thermal mismatch between fiber and matrix and a slight thermochemical damage of fiber during the densification. The addition of interfacial coating is able to adjust the thermal stress and protect fiber from thermochemical damage, thus weakening interfacial bonding and improving fracture toughness of composites. This will be investigated in subsequent work.

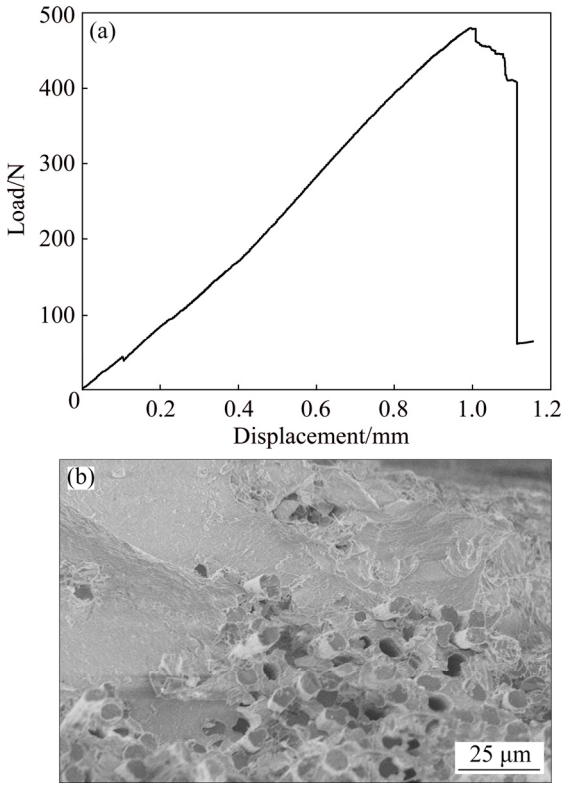

Fig. 7 Load−displacement curve (a) and fracture surface (b) of as-received C/mullite composites

The as-received C/mullite composites were oxidized at 1200, 1400 and 1600 °C for 30 min to characterize oxidation resistance. The mass loss and the mechanical properties retention after oxidation are listed in Table 1. As mentioned above, there are some open pores (12%) and microcracks in composites. It is easy for oxygen to diffuse into composites through these pores and microcracks and oxidize carbon fibers, leading to mass loss and degradation in mechanical properties. When oxidation at 1200 °C, the microcracks derived from thermal stress cannot be completely healed since the as-received composites were fabricated at 1400 °C. As a result, the maximum mass loss of 4.5% and the minimum modulus retention ratio are detected. The fact that the strength retention ratio at 1200 °C is not the lowest is probably related with the random oxidation of carbon fibers. Maybe, the oxidized carbon fibers do not bear much load. Owing to the healing of microcracks, the mass loss is remarkably decreased and the modulus retention ratio is notably improved at 1400 °C. When the oxidation temperature was elevated to 1600 °C, solid state sintering of the mullite and the rich SiO_2 is active, as reflected by the linear shrinkage in Fig. 4. The solid state sintering promotes further densification of the matrix, healing some open pores and microcracks and improving capacity of bearing load. By comparing Fig. 6 and Fig. 8, it is clear that the oxidation at 1600 °C has little influence on the microstructure of C/mullite composites and the disappear of carbon fiber due to oxidation is not observed. Accordingly, the mass loss becomes tiny and the mechanical properties are almost unchanged after oxidation.

Table 1 Mass loss and mechanical properties retention of C/mullite composites after oxidation

Oxidation temperature/°C	Mass loss/%	Flexural strength retention/%	Flexural modulus retention/%
1200	4.5	84.3	74.2
1400	2.4	84.0	90.6
1600	0.6	101.9	96.3

The tiny mass loss and the unchanged strength and modulus suggest that the carbothermal reaction between fiber and matrix is not activated at 1600 °C. This means that oxidation at this temperature does not strengthen the chemical bonding of interface. However, the physical bonding of interface is enhanced due to the sintering shrinkage of matrix. Thus, as illustrated in Fig. 9, the maximum displacement at invalidation point is reduced from ~1 mm before oxidation to ~0.9 mm after oxidation at 1600 °C.

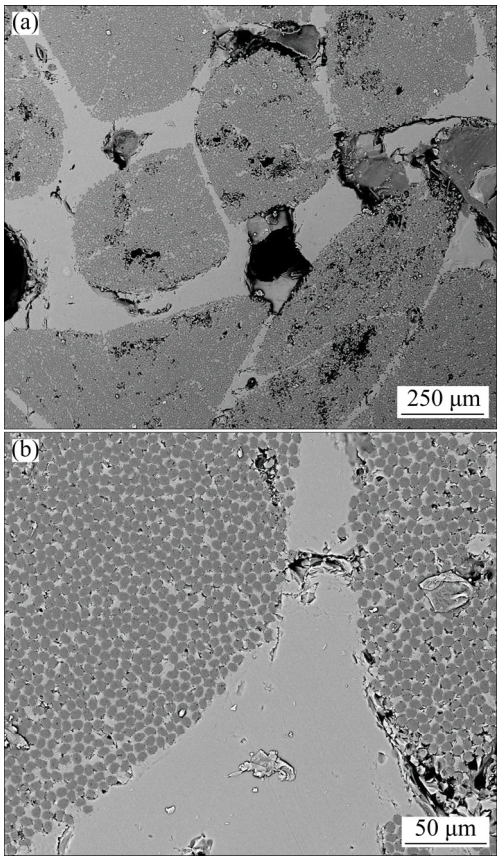

Fig. 8 SEM images of transverse section of C/mullite composites after oxidation at 1600 °C

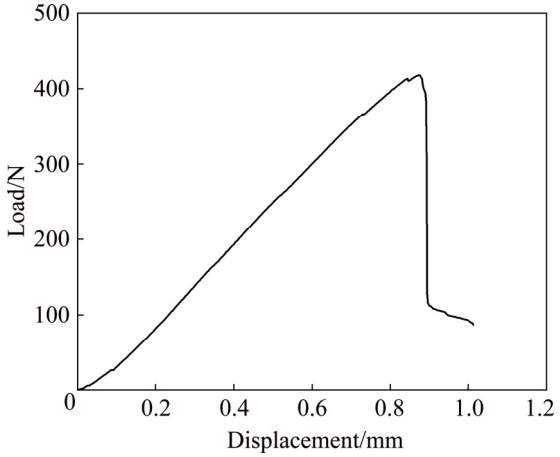

Fig. 9 Load−displacement curve of C/mullite composites after oxidation at 1600 °C

4 Conclusions

1) The Al_2O_3−SiO_2 diphasic sol with a solid content of 20% (mass fraction) and an Al_2O_3/SiO_2 mass ratio of 2:1 is the proper raw material for the fabrication of three-dimensional braided carbon fiber reinforced mullite (3D C/mullite) composites. The mullitization is basically completed at 1300 °C and the Al_2O_3−SiO_2 gel shows favorable sintering shrinkage.

2) The 3D C/mullite composites are fabricated through the route of vacuum impregnation−drying−heat treatment. Even if the total porosity reaches 26.0% and there is no interfacial coating, the composites show favorable mechanical properties and non-catastrophic fracture behavior.

3) Benefiting from the further densification of matrix, the 3D C/mullite composites exhibit tiny mass loss and their mechanical properties are well retained after oxidation at 1600 °C for 30 min.

References

[1] SCHNEIDER H, SCHREUER J, HILDMANN B. Structure and properties of mullite—A review [J]. Journal of the European Ceramic Society, 2008, 28: 329−344.

[2] LIANG Shu-quan, ZHONG Jie, TAN Xiao-ping, TANG Yan. Mechanical properties and structure of zirconia−mullite ceramics prepared by in-situ controlled crystallization of Si−Al−Zr−O amorphous bulk [J]. Transactions of Nonferrous Metals Society of China, 2008, 18: 799−803.

[3] MA Bei-yue, LI Ying, CUI Shao-gang, ZHAI Yu-chun. Preparation and sintering properties of zirconia−mullite−corundum composites using fly ash and zircon [J]. Transactions of Nonferrous Metals Society of China, 2010, 20: 2331−2335.

[4] KUMAR P, NATH M, GHOSH A, TRIPATHI H S. Thermo-mechanical properties of mullite−zirconia composites derived from reaction sintering of zircon and sillimanite beach sand: Effect of CaO [J]. Transactions of Nonferrous Metals Society of China, 2016, 26: 2397−2403.

[5] WANG Yi, LIU Hai-tao, CHENG Hai-feng, WANG Jun. Effective fugitive carbon coatings for the strength improvement of 3D Nextel^{TM} 440/aluminosilicate composites [J]. Materials Letters, 2014, 126: 236−239.

[6] WANG Yi, CHENG Hai-feng, WANG Jun. Effects of the single layer CVD SiC interphases on mechanical properties of mullite fiber-reinforced mullite matrix composites fabricated via a sol−gel process [J]. Ceramics International, 2014, 40(3): 4707−4715.

[7] WANG Yi, LIU Hai-tao, CHENG Hai-feng, WANG Jun. Effects of sintering temperature on mechanical properties of 3D mullite fiber (ALF FB3) reinforced mullite composites [J]. Ceramics International, 2013, 39(8): 9229−9235.

[8] KAYA C, BUTLER E G, SELCUK A, BOCCACCINI A R, LEWIS M H. Mullite (Nextel^{TM} 720) fibre-reinforced mullite matrix composites exhibiting favourable thermomechanical properties [J]. Journal of the European Ceramic Society, 2002, 22: 2333−2342.

[9] COLOMBAN Ph, BRUNETON E, LAGRANGE J L, MOUCHON E. Sol−gel mullite matrix−SiC and mullite 2D woven fabric composites with or without zirconia containing interphase: Elaboration and properties [J]. Journal of the European Ceramic Society, 1996, 16: 301−314.

[10] WU J, JONES F R, JAMES P F. Continuous fibre reinforced mullite matrix composites by sol−gel processing. Part I: Fabrication and microstructures [J]. Journal of Materials Science, 1997, 32(13): 3361−3368.

[11] WU J, JONES F R, JAMES P F. Continuous fibre reinforced mullite matrix composites by sol−gel processing. Part II: Properties and fracture behaviour [J]. Journal of Materials Science, 1997, 32(14): 3629−3635.

[12] DONG R, HIRATA Y, SUEYOSHI H, HIGO M, UEMURA Y. Polymer impregnation and pyrolysis (PIP) method for the preparation of laminated woven fabric/mullite matrix composites with pseudoductility [J]. Journal of the European Ceramic Society, 2004, 24: 53−64.

[13] XIANG Yang, WANG Qing, CAO Feng, MA Yin-wei, QUAN Dong-liang. Sol−gel process and high-temperature property of SiO_2/ZrO_2−SiO_2 composites [J]. Ceramics International, 2017, 43(1): 854−859.

[14] WANG Qing, CAO Feng, XIANG Yang, PENG Zhi-hang. Effects of ZrO_2 coating on the strength improvement of 2.5D SiC_f/SiO_2 composites [J]. Ceramics International, 2017, 43(1): 884−889.

[15] BERAN A, VOLL D, SCHNEIDER H. Dehydration and structural development of mullite precursors: an FTIR spectroscopic study [J]. Journal of the European Ceramic Society, 2001, 21: 2479−2485.

[16] CIVIDANES L S, CAMPOS T M B, RODRIGUES L A, BRUNELLI D D, THIM G P. Review of mullite synthesis routes by sol−gel method [J]. Journal of Sol-Gel Science and Technology, 2010, 55: 111−125.

基于高固相含量溶胶制备三维编织碳纤维增强莫来石复合材料

张 伟[1,2]，马青松[2]，戴科伟[2]，毛卫国[1]

1. 湘潭大学 材料科学与工程学院，湘潭 411105；

2. 国防科技大学 新型陶瓷纤维及其复合材料重点实验室，长沙 410073

摘 要：以固相含量为 20%(质量分数)、Al_2O_3/SiO_2 质量比为 2:1 的 Al_2O_3−SiO_2 溶胶为原料，制备三维编织碳纤维增强莫来石(3D C/mullite)复合材料。分析溶胶的特性与莫来石化行为，发现溶胶经 1300 °C 热处理基本实现完全莫来石化，凝胶粉呈现出较好的烧结收缩特性。通过溶胶“真空浸渍－干燥－热处理”路线制备出 3D C/mullite 复合材料，即使总孔隙率为 26.0%，复合材料仍获得良好的力学性能，弯曲强度和断裂韧性分别为 241.2 MPa 和 10.9 MPa·$m^{1/2}$。表征复合材料在 1200、1400 和 1600 °C 下的抗氧化性能。由于基体的进一步致密化，3D C/mullite 复合材料在 1600 °C 下氧化 30 min 后，仅有微小的质量损失，力学性能几乎没有变化。

关键词：碳纤维增强莫来石复合材料；Al_2O_3−SiO_2 溶胶；力学性能；抗氧化性能

(Edited by Bing YANG)